applied sciences

MDPI

Article

Determination of Forest Structure from Remote Sensing Data for Modeling the Navigation of Rescue Vehicles

Marian Rybansky

Faculty of Military Technology, University of Defence, Kounicova 65, 662 10 Brno, Czech Republic; marian.rybansky@unob.cz; Tel.: +420-973-445-298

Abstract: One of the primary purposes of forest fire research is to predict crisis situations and, also, to optimize rescue operations during forest fires. The research results presented in this paper provide a model of Cross-Country Mobility (CCM) of fire brigades in forest areas before or during a fire. In order to develop a methodology of rescue vehicle mobility in a wooded area, the structure of a forest must first be determined. We used a Digital Surface Model (DSM) and Digital Elevation Model (DEM) to determine the Canopy Height Model (CHM). DSM and DEM data were scanned by LiDAR. CHM data and field measurements were used for determining the approximate forest structure (tree height, stem diameters, and stem spacing between trees). Due to updating the CHM and determining the above-mentioned forest structure parameters, tree growth equations and vegetation growth curves were used. The approximate forest structure with calculated tree density (stem spacing) was used for modeling vehicle maneuvers between the trees. Stem diameter data were used in cases where it was easier for the vehicle to override the trees rather than maneuver between them. Although the results of this research are dependent on the density and quality of the input LiDAR data, the designed methodology can be used for modeling the optimal paths of rescue vehicles across a wooded area during forest fires.

Keywords: forest fire; rescue vehicle; vegetation structure; optimal pathfinding; canopy height model (CHM)

Citation: Rybansky, M. Determination of Forest Structure from Remote Sensing Data for Modeling the Navigation of Rescue Vehicles. *Appl. Sci.* **2022**, *12*, 3939. https://doi.org/10.3390/app12083939

Academic Editors: Giovanni Randazzo, Stefania Lanza and Anselme Muzirafuti

Received: 22 March 2022
Accepted: 11 April 2022
Published: 13 April 2022

1. Introduction

Forest fires are very frequent crisis situations, especially in dry or arid landscapes [1]. The prediction of forest fire occurrence depends on knowledge of the factors that affect the fires and on the technologies that facilitate the monitoring and modeling the spread of the fire. Ganteaume et al. [2] analyzed the most common human and environmental factors driving forest fire ignition. The primary factors that directly cause forest fires are natural (lightning strikes, seismic and volcanic activity, etc.) or human (carelessness and activities such as arson, slash-and-burn agriculture, fire-fallow cultivation, machinery sparks, discarded glass bottles or cigarette butts, military activity, etc.). The factors that determine fire spread are as follows: forest type and structure (distances between trees, *DBH*, canopy height, tree crown density, etc.); meteorological conditions (precipitations, temperature, wind speed, air humidity, cloudiness, soil moisture, etc.); topographic (morphological shapes of terrain, orientation of relief slopes, etc.); geological and pedological (underground structure, soil structure, and terrain surface color); and season and time of day, which determine the amount of available sunlight and temperature, etc. The technologies that facilitate the monitoring and modeling of a forest structure and the spread of forest fires include the sensor types for vegetation data collection and forest structure determination and technologies for monitoring and modeling the spread of fire. Blair, Rabine, and Hofton [3] described the Laser Vegetation Imaging Sensor (LVIS), which operates at altitudes of up to 10 km aboveground and is capable of producing data for topographic mapping with dm accuracy and vertical height and structure measurements of

vegetation. The LVIS instrument is also suitable for subcanopy ground elevation mapping. Lim et al. [4] described many of the initial studies of the application of LiDAR for forestry focused on verifying through statistical analysis that LiDAR could be used to accurately measure forest attributes. The focus has been on canopy tree heights given the nature of this attribute as a predictor variable for other forest attributes, such canopy density. Hyyppä et al. [5] analyzed existing algorithms and methods of airborne laser scanning that are used for extraction of the canopy height and individual tree information. Aschoff and Spiecker [6] described an algorithm for detecting trees in a semiautomatic way. Gobakken and Næsset [7] analyzed the effects of forest growth on laser-derived canopy metrics. Carson et al. 2004 [8], Ahlberg et al. [9], and Su et al. [10] provided the overview of LiDAR applications in forestry. By comparing these methods based on laser scanning, it can be stated that, at present, an approximate forest structure for modeling the movement of rescue vehicles can be determined. At the metric density of the DSM (CHM), the error in tree positioning can reach values in decimeters, sometimes up to meters, depending on the structure and type of the canopy. At the decimeter density of the DSM points out, it is possible to calculate the tree position errors in centimeters to decimeters. When comparing the possibilities of using LiDAR and aerial optical images, both methods have advantages and disadvantages. Aerial images provide both spatial and image information, but they do not allow, unlike LiDAR, full automation to determine the forest structure.

However, the use of LiDAR and aerial optical images may be problematic in the area of fire because of the clouds or smoke generated by the fire. In these situations, radar methods can be used to measure forest parameters. The mapping of forest units by radar is described, for example, by Martoni et al. in [11]. Kugler et al. [12] compared the LiDAR and radar methods for determining the heights of the forest in three areas: boreal, temperate, and tropical. The correlations achieved confirm the possibility of combining the use of both forest mapping methods. Additionally, Cazcarra-Bes et al. [13] described the possibilities of the horizontal and vertical forest structure mapping from radar using data obtained by synthetic aperture radar tomography. The use of radar methods is, however, limited in terms of the accuracy of the determination of the characteristics of individual trees. Furthermore, Landsat or Sentinel 2 global satellite data can be used to monitor forests before and during a fire. Sentinel 2 with a multispectral instrument (MSI) with 13 spectral channels in the visible/near-infrared (VNIR) and shortwave infrared spectral range (SWIR) and three bands for vegetation mapping can provide the crisis management with actual data in the shortest possible time, especially during a forest fire. The data accuracy (about 20 m) does not allow a more accurate mapping of the internal forest structure—see, e.g., Puletti et al. [14].

Technologies for monitoring and modeling the spread of a fire are divided into stages: prediction, during the fire, and post-fire [15]. Milz and Rymdteknik [16] described the technologies of detection and the spread of the forest fires by using satellite-borne remote sensing techniques. However, the technologies of fire monitoring and distribution are limited by the availability of up-to-date data from satellites, planes, UAVs, or terrestrial observations. We also need to know the prediction of the spread of a fire to deploy rescue vehicles. Koo et al. [17] described possible solutions using a physical model for the forest fire spread rate. This model successfully evaluated wind and slope effects of a fire on forest vegetation.

The above-mentioned factors and technologies are very important for the teams (fire brigades, military units, health services, and police) that are deployed to rescue people and reduce the damage during forest fires. Remote sensing support is very important for rescue units when they are moving across vegetation before and during a fire and, also, for the decision to deploy aircraft. We can use LiDAR and aerial image data to create a navigation analysis for rescue (fire brigade or military) vehicles—see also [18–20]. These data can be supplemented by active fire scenes using infrared sensors or aerial or UAV images. Among the most effective data sources for Cross-Country Movement (CCM) navigation and optimal pathfinding across a forest are LiDAR data and the products of its analysis.

A prerequisite for the success of this analysis is an up-to-date picture of vegetation data obtained by laser scanning. This precondition is especially crucial for forest stands, where data become quickly outdated due to vegetation growth.

The primary focus of this article was the LiDAR data update for the forest stand structure, a simulation of the creation of a forest structure with the subsequent creation of a model for navigating the movement of a rescue vehicle between trees as obstacles in the terrain. The reason for designing the method of detecting the current forest structure was that LiDAR data in the Czech Republic is gradually becoming obsolete as a result of tree growth. The following procedure was chosen: (1) Selection of the most common type of forest stands in the territory of the Czech Republic with the predominant spruce tree (Picea abies). Obtaining LiDAR data characterizing DSM with a density of 1 × 1 m. (2) Obtaining inventory data on the growth of spruce trees from MENDEL University, Brno. (3) Detection of DSM accuracy by geodetic and photogrammetric method. (4) Corrections of tree heights due to DSM density and tree growth. (5) Creation of forest structure by random distribution. (6) Selecting a simulated area where a fire could occur (older, drier forest). (7) Calculating the simulated shortest route for a particular vehicle (outside the area of the fire). The research results presented in this paper represent a new methodology of updating a digital surface model (DSM) or canopy height model (CHM) using the equations of tree growth and vegetation growth curves. DSM and Digital Elevation Model (DEM) data evaluated for forestry passability were scanned by LiDAR in 2013. CHM data and field measurements were used for determining the approximate forest structure (tree height, *DBH*, and stem spacing between trees). The described methods were tested on a spruce forest stand composed only from one type of tree—Sitka spruce (Picea abies), situated approximately 300 m south of the village of Brno-Utechov (see Figure 1), where the heights of trees in the Krtiny Training Forest Enterprise (TFE) area were detected and measured. This spruce forest was chosen because of the availability of a series of aerial photos and LiDAR data. Additionally, the forest is highly representative, as it contains the tree species most commonly found in many Central European countries. The current age of this forest is about 30 years.

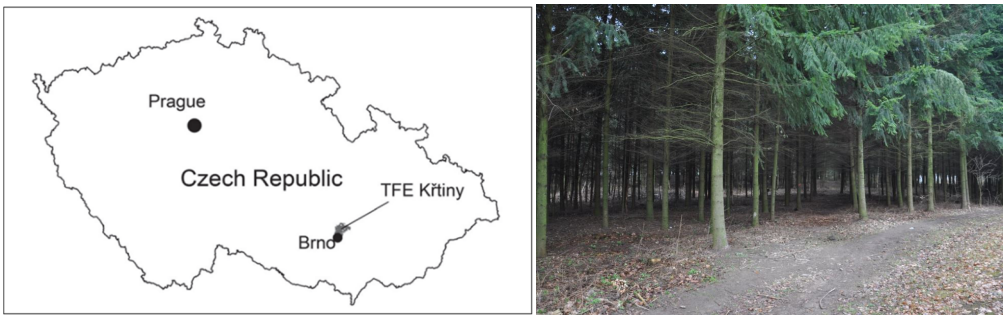

Figure 1. Location and character of TFE Krtiny.

The approximate forest structure with the calculated tree density (stem spacing) was used for modeling fire brigade vehicle maneuvers between the trees. *DBH* data were used in cases where it was easier for the vehicle to override the trees rather than maneuver between them. *DBH* data were also used for the calculation of the distances between trees. Due to the availability of a DSM with a density of 1 × 1 m, it was impossible to precisely determine the locations of individual trees, so a random simulated forest structure was created based on the number of trees per hectare.

The article describes the methodology of calculation of the rescue vehicle movement using simulated areas of a burning forest. In the case of a real fire, we can use the above-mentioned LiDAR data (DSM data) or current data from different sensors. The type of sensors and the accuracy of the data obtained will have a significant impact on the terrain analysis and search algorithm for optimal rescue vehicle routes. Only some scattered and low-resolution data of the fire can help. If the optimal route for a special vehicle

(fire-resistant rescue vehicle, tank, etc.) that will move through a burning forest is to be calculated, we will need detailed vegetation and elevation data with a meter or decimeter resolution for reconnaissance of fallen trees, boulders, etc.

2. Materials and Methods

Interventionary studies involving animals or humans, and other studies that require ethical approval, must list the authority that provided approval and the corresponding ethical approval code. For modeling forest passability for fire brigade vehicles, it was first necessary to specify a forest structure using the DSM of a forest created from a LiDAR data source using DEM, photogrammetric method, and tachymetry to correct the tree heights. In order to update the CHM and determine the above-mentioned forest structure parameters, tree growth equations and vegetation growth curves were used. However, DSM forest data change quite rapidly, so it was necessary to adjust the CHM and forest structure model. Having an updated forest structure, we finally created a model of its passability by a chosen fire brigade vehicle Tatra 815.

2.1. Forest Structure Determination

The most important elements of forest structure determination for modeling vehicle passability across vegetation are the average distances between trees and *DBH*. When determining the forest structure while not using the most recently acquired LiDAR data, it can be assumed that the older trees are taller (see [21–24] and Figure 2), the diameter of the trunks grow, the distances and between trees also grow over time, but the number of trees per unit area decreases. In order to derive the age, distances, and *DBH* of trees from their height, a homogeneous forest, composed only from one type of spruce, was chosen. All following equations and vegetation growth curves were provided by the Mendel University in Brno and obtained from inventory data.

The number of trees per square unit N·ha-1 depends on the age of vegetation, slope and other parameters (see Fatehi et al. [25]). We can express it using Formula (1) [26,27]:

$$N = B \cdot t^{-m}, \quad (1)$$

where B and m are the constants of vegetation stand quality, and t is an age.

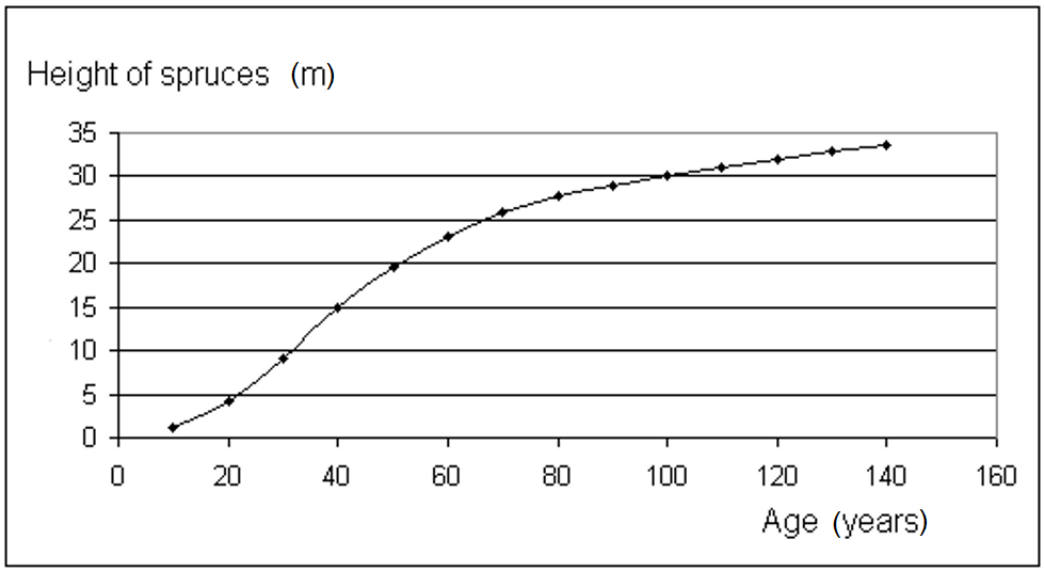

Figure 2. Process of height growth of a spruce forest [28].

When we know the age of the vegetation (which can be derived from the height) we can determine the number of trees per hectare (N)—see [21]. The number of trees per unit area is also highly important for determining the average distances between trees

within a given forest unit—Mean Tree Spacing (*MTS*). We can express the *MTS* using Formula (2) [21,28]:

$$MTS \cong \sqrt{\frac{40,000}{\pi \cdot N}} - MDBH \quad (2)$$

where *N*—number of trees per 1 ha, and *MDBH*—mean *DBH*.

The last important element of forest structure is *DBH*. Tree trunks are measured at the height of an adult's breast. However, this is defined differently in different countries and situations. The convention is now 1.3 m above ground level. The *DBH* of trees is a function of the *N*—number of trees per 1 ha, the age of vegetation, slope, and other parameters. We can express it using Formula (3):

$$N = B \cdot DBH^{-k}, DBH = (N/B)^{k} \quad (3)$$

where *B* and *k* are the constants of the vegetation stand quality. Each type of tree has its own constant *B* and *k*—see also [26].

All of the above-described methodology defining the relationships between forest structure parameters were applied in the context of obsolete LiDAR data acquired in 2013. The procedure for determining the individual parameters of the forest structure is shown in Figure 3.

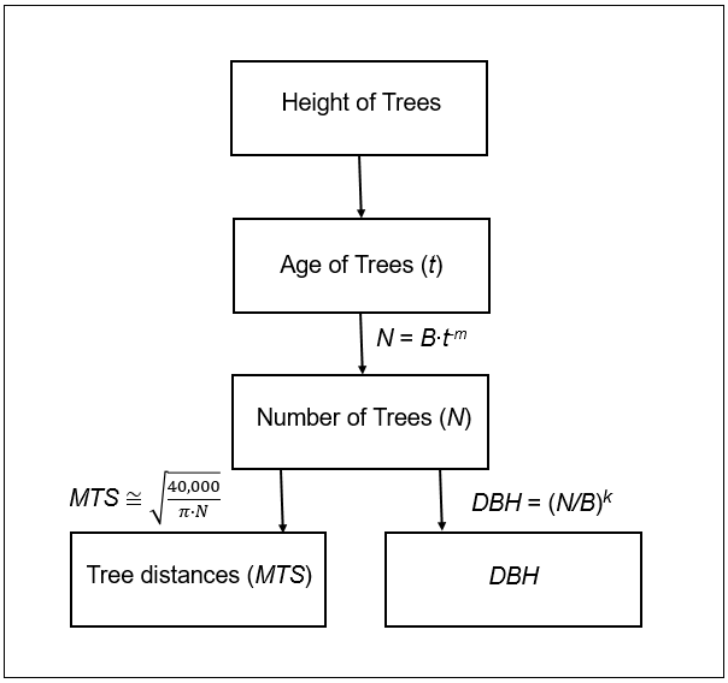

Figure 3. Dependence of forest structure determination.

The heights of the trees are extracted from LiDAR or DSM data. The ages of trees are possible to determine from the inventory data or from the growth equations and parameters. Additionally, the number of trees and *DBH* can be directly determined from the inventory data or calculated from *N*.

2.2. Forest Structure Updating

For determining the CHM while not using the most recently acquired LiDAR data (from 2013), it was necessary to recalculate the tree height according to spruce age—see Figure 2 and Formula (1). For determining the forest structure parameters, LiDAR data and the derived DSM (CHM) were used. Since the default DSM data density was 1 m × 1 m, it was necessary to verify how the actual spruce heights differ from the heights determined by the DSM. Verification was done using a photogrammetric evaluation of the aerial

photographs and geodetic method (tachymetry) for accuracy verification—see also [21]. Geodetic measurements of the positions of 116 trees and their heights were carried out by a total station Leica TC 1500. Geodetic survey of the tree heights was taken as the most accurate measurement method. Those tree height estimations were determined photogrammetrically in different time periods with the aid of color aerial photographs. The Military Geographical and Hydrometeorological Office (VGHMÚř) Dobruška took them at regular photographing periods in the Czech Republic (2003, 2006, 2009, 2012, and 2014). A detailed description of the photogrammetric evaluation was given in [21]. Tree height LiDAR data do not match those more accurate from aerial photographs due to the fact that the density of the reflected laser beams (1 m × 1 m) is not sufficient enough to catch the peaks of trees—see the red dots in Figure 4. The LiDAR average tree height is 6 m less than the average height determined by the photogrammetric method [22]. Photogrammetric evaluation and tachymetric verification revealed that, because of the lower density of the LiDAR data (1 m × 1 m), the treetops were not captured, and DSM needed to be corrected (increase in height)—see the red lines in Figure 4.

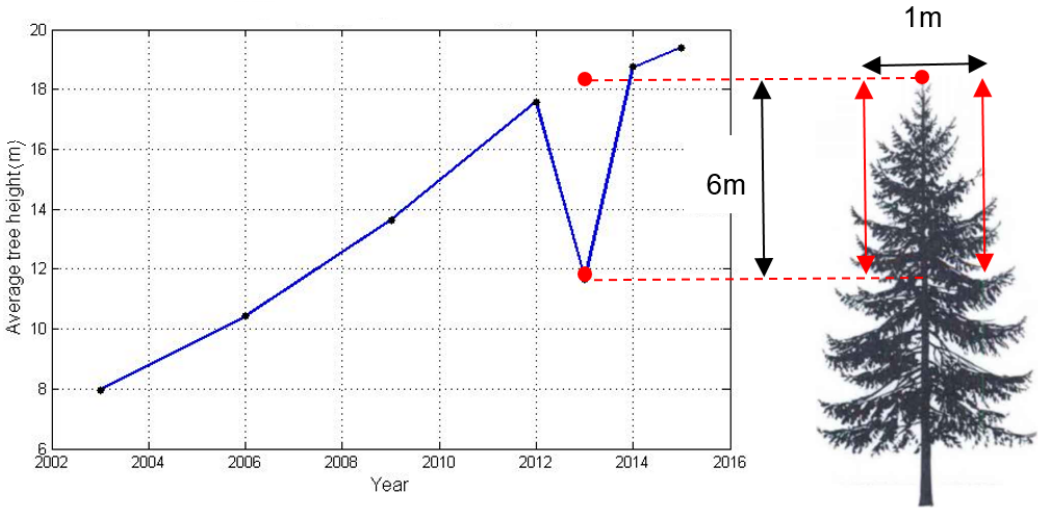

Figure 4. Dependence of a forest structure determination.

Figure 4 shows a series of average spruce heights from 2003, 2006, 2009, 2012, and 2014 determined for the photogrammetry (blue points) and the average height of the same forest determined from the DSM in 2013 from the LiDAR data (red point). The height difference for 2013 was about 6 m; that is, we needed to adjust the values of the DSM heights (CHM) for this constant. Due to the corrected elevations of the DSM, it was possible to define a new forest structure (see the methodology above) and calculate the tree distances and stem diameters. For the forest structure simulation, the normal Gauss distribution of distances and *DBH* were used. The mean values of height, distance, and *DBH* were used at 18 m, 4 m, and 0.25 m.

2.3. Passability Model

To find the optimal route through the forest, it is necessary to know: parameters of the vehicle, parameters of the trees, start and end points of a route, and impassable areas. The most important parameters of a vehicle are vehicle width (*VW*), length, turning radius, and tolerance (*T*)—see Figure 5.

(**a**) (**b**)

Figure 5. Fire and tested vehicles. (**a**) Fire vehicle Tatra 815 4 × 4, Length/Width/Height: 7950/2550/3000 mm. (**b**) Tested terrain vehicle Tatra 815 8 × 8, Length/Width/Height: 8950/2550/3300 mm.

T determines the minimum distance of the vehicle from a trunk to pass between two trees safely. To simplify the passability model, *T* also replaces the effect of other vehicle parameters (length, turning radius, etc.). In turn, tree parameters refer to those characteristics that are key to finding the optimal route in the forest. In our case, those parameters are stem simulated coordinates, mean tree spacing (*MTS*), mean *DBH*, mean riding corridor (*MRC*), and a *VW*. We can express the relationship between *MTS*, *MDBH*, and *MRC* (see Figure 6) using Formula (4):

$$MRC = MTS - MDBH. \quad (4)$$

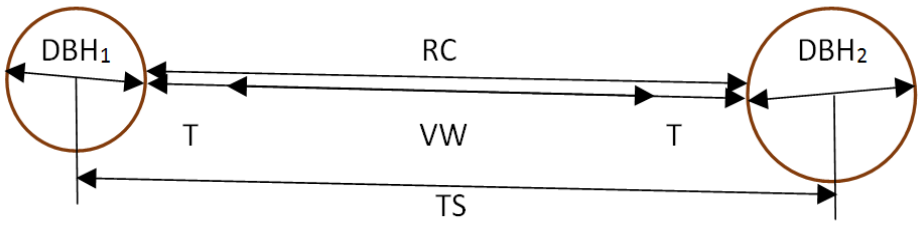

Figure 6. The relationship between particular tree spacing, *DBH*, and riding corridor.

If we do not know the exact coordinates of each tree (which is the usual situation), we can generate the simulated forest structure from average values—see the procedure above. We use the process of random tree deployment to determine the probability of crossing the forest.

The start and end points of a route can be substituted by an initial and final area in a forest region. It is usually not possible to go between these points or areas directly, and we must maneuver between tree stems. Impassable objects (steep slopes, rocks, lakes, rivers, burning forest, etc.) can be obtained from GIS databases or using aerial or satellite images. For the purposes of modeling vehicle mobility in the above-described forest, the impassable areas of the simulated burning polygons were chosen, though other objects (obstacles) were not considered. To search the optimal vehicle route, the following algorithms were used (see Figure 7): Voronoi graph and Delaunay triangulation, Dijkstra algorithm, and optimization of the fractional line.

Figure 7 shows the positions of individual trees (Vertex M)—blue points. The closest two trees to the given tree create the Delaunay triangle—Figure 7b, and the most secure route sections (Voronoi edges) are intersected in the Voronoi nods—blue lines in Figure 7c. The Dijkstra algorithm was used to find the shortest routes from the nod of the graph given to all other nods—see also [23,24]. Using Figure 7c, we can simulate a forest path (see Figure 7d). Trees that were obstacles are marked in red, and Voronoi nods (pale blue points) are connected with Voronoi edges (dark blue lines). All Voronoi edges are rated by weights. These weights may represent the distances or time for which a vehicle passes through the Voronoi edges. In the event that we search for the shortest route from point 1 to point 15, the condition of the minimum sum of the Voronoi edges (weighing) is to be compliant with

the shortest route—red line in Figure 7d passing through Voronoi nods 1-3-7-6-11-12-14-15, since the sum of route segment values (3.0 m + 3.3 m + 0.8 m + 3.8 m + 1.2 m + 2.1 m + 1.6 m) = 15.8 m is the smallest (shortest) compared to all possible routes connecting points 1 and 15.

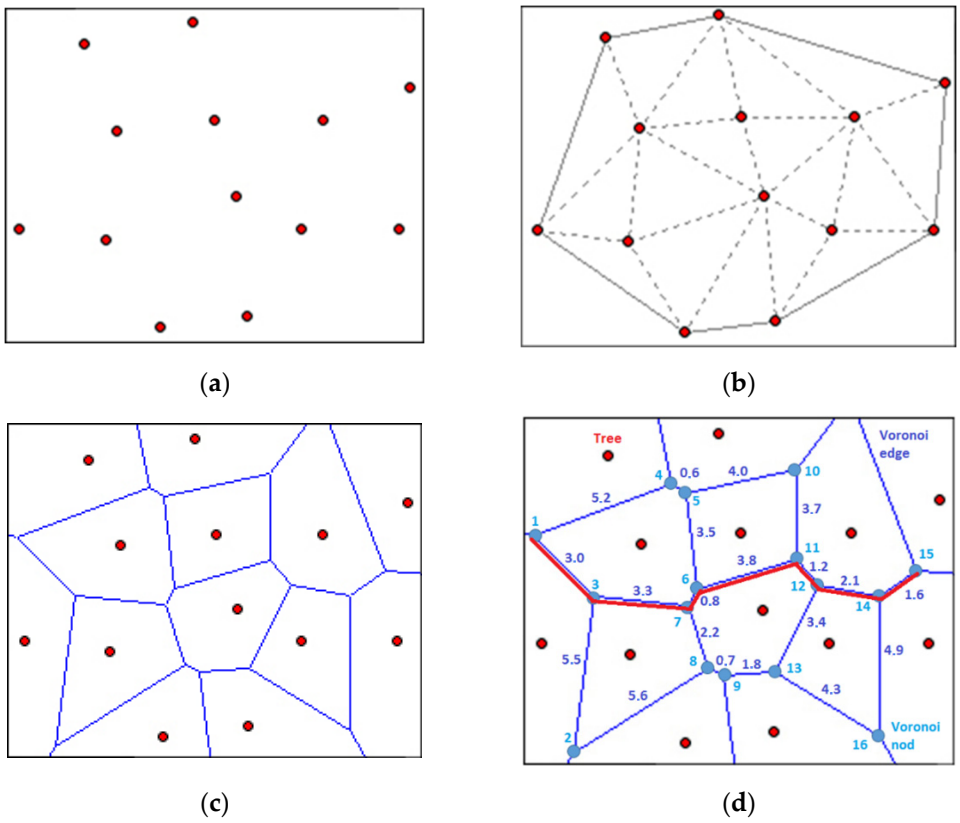

Figure 7. The relationship between the Delaunay triangulation and Voronoi graph (scale 1:200). (**a**) Set of trees generated from average *MTS* values. (**b**) The area is divided into elementary triangles using Delaunay triangulation (each reference tree has its two closest neighbors). (**c**) Axes of triangle sides create so-called Voronoy edges and Voronoy cells. (**d**) Voronoy edges represent the safest.

3. Results

The result of the creation of a forest structure from data obtained from the original forest (see Figure 8) by generating random tree positions is shown in Figure 9. The size of the analyzed forest area was 140 × 80 m (11,200 m^2). The length of the vehicle's passage was 212 m. The direct path between the starting point and the target is shown by a black line. This path is generally unrealistic due to the tree stem obstacles (displayed as green points). All possible paths (blue closed Voronoi polygons) that match the tree distances and vehicle parameters have been computerized using Dijkstra algorithm and displayed in Figure 8 using our own software tools. Unfinished Voronoi polygons (ending between trees) are nonbinding paths where the width of the vehicle does not allow passage between trees. We can choose any of these blue passable routes, but only one will be the shortest (fastest)—the red highlighted route. This route traverses around (between) the burning forest polygons. The simulation of the polygons displaying the fire areas was done completely at random by adding the points around the impassable zones (orange areas). These areas can be complemented e.g., by satellite images or aerial photos. If we wanted to avoid these risky places, we would have to create a security zone around the burning polygons—so-called buffers—using GIS tools.

Figure 8. The Sitka spruce forest near Utechov, where the heights of trees and *DBH* data were measured (scale 1:1000, center coordinates: φ = 49.282744, λ = 16.632918)—(Ortophoto Mapy.cz).

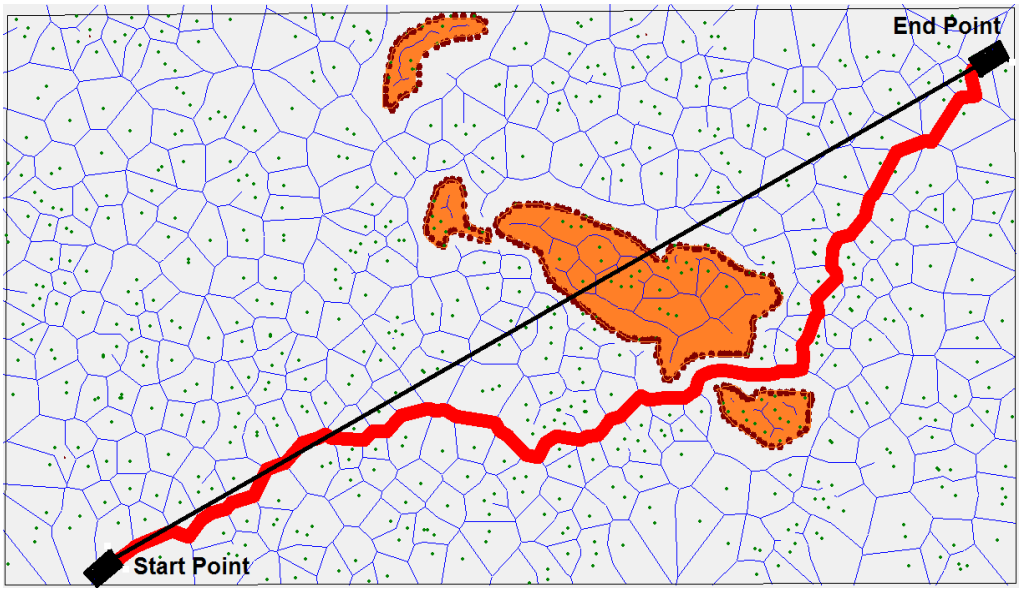

Figure 9. Navigation on the shortest vehicle route (red track) avoiding the burning forest (orange areas). Randomly spaced trees, approx. scale 1:1000.

There are also displayed the routes inside the areas of fires (blue lines inside the orange polygons)—see Figure 9. These routes can be used later when the fires end, but they are primarily not included into the calculation of the shortest route. For some types of vehicles, such as tanks, we can also choose the route through the burning area and calculate the route segments inside the orange polygons. The influence of other elements of the terrain (slope gradient, soil properties, terrain surface roughness, forest paths, etc.) are not calculated.

The above-mentioned result of seeking an optimal forest path partially affected by a fire may be modified in case when the forest structure is regular triangular or rectangular. There are displayed all the possible routes and the shortest route—red line in the triangular forest structure in Figure 10.

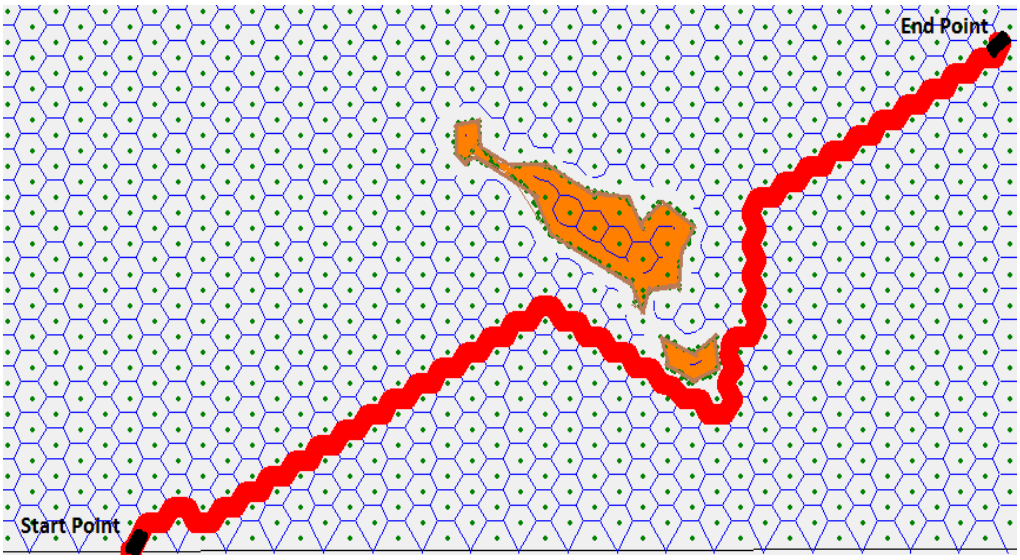

Figure 10. Navigation on the shortest vehicle route—regular triangular forest structure—scale 1:1500.

The methodology for finding the optimal rescue vehicle path was based on verifying the input data. Determining a forest structure from DSM data can be very unreliable, especially when LiDAR data are obsolete. Therefore, the use of growth curves of trees and derived vegetation parameters were used. These parameters were determined on a relatively small area. Verification of the vegetation parameters by photogrammetric and geodetic pathways lasted several months. The results of the presented model are valid for the designated coniferous forest. The general application of the optimal vehicle route determination will depend on the type of trees (coniferous, deciduous, and mixed). The author assumes that the presented model for finding the optimal route of a vehicle will be better utilized with the development of mapping methods aimed at determining the exact coordinates of the trees.

4. Discussion

The described methodology for determining the possibility of moving the fire brigade vehicles in forest vegetation can be used if tree position data or forest structure (generated from photogrammetric data or from LiDAR data) are available. In both cases, the same algorithm can be used to find the optimum forest path. In case we have more precise tree coordinates (from terrestrial or remote sensing sensors), the calculated route of the vehicle will be more reliable. Although the methods of directly determining the exact tree position by remote sensing data are constantly developing, the forest structure is often determined using DSM (CHM) methods. This is due to the financial cost of the high density of LiDAR data, as well as the personnel demand for data acquisition using photogrammetric methods. The quality of the photogrammetric evaluation depends on the scale of the images and the evaluator's experience. The main problem is to target the marker at the tree's top point, which is above the tree trunk. The accuracy of tree position evaluation is higher for coniferous trees than for leafy vegetation. The disadvantage of the photogrammetric method is the lower performance of manual evaluation compared to the possibility of automated evaluation of LiDAR data. LiDAR methods are faster than photogrammetric methods, and they allow a more efficient assessment of the forest structure and determination of the possibilities of vegetation passability without a manual evaluation. LiDAR methods can also be better combined with other remote sensing data sources (infrared, multispectral, radar, etc.). For example, an infrared spectrum can be used to map environmental and fire temperature characteristics, and at night, multispectral imagery can be used to classify species, and radar data is appropriate for mapping a burning forest covered with smoke or clouds. However, these methods have a disadvantage when

scanning vegetation with a low density of DSM elevation points (smaller than 1 m × 1 m) and in the case of DTM data absence. On the other hand, the repeated photogrammetric evaluation of the representative forest stands and the data from DSM could bring about a new approach for forest growth analysis and could be a sufficient method for DSM updating in different growth conditions of forest stands.

The results of this experiment showed that this method is fully applicable for the DSM generated from LiDAR data. The method can be appropriately implemented as a relatively inexpensive updating tool for GIS technology between two laser scanning campaigns of a territory. This method can also be refined using the growth curves of individual types of trees. Forest growth characteristics are very important due to the age of LiDAR DSM data. The results of photogrammetric measurements from aerial images taken at consecutive time intervals and statistical calculations show that the growth curves of the trees are initially steeper, but vegetation growth later slows. It is also necessary to investigate the relationships between the natural environment factors and specific canopy growth. The above-mentioned DSM updating method could be used for many applications, e.g., in forestry, military, etc.—see, e.g., [29–33]. It should be noted that the tree height correction values decrease with the increasing density of the LiDAR data. At the DSM density 1 m × 1 m, the average correction is approx. +6 m. At the DSM points density of 1 dm × 1 dm, it is possible to estimate the average height corrections of spruce trees in decimeters, depending on the age of the vegetation. Height corrections of the DSM can significantly affect the computationally generated forest structure and, hence, the vehicle motion models. The resulting model of forest crossing by a vehicle will depend, to a large extent, on the quality of the forest structure data. This study focused on a spruce forest—the predominant tree species in Central Europe. In general, it can be said that the species of vegetation may be variable in different forest groups. From this point of view, the study presented in this article can be considered as partially applicable. Using LiDAR/DSM data, the determination of the deciduous forest structure and positioning of the tree trunks will be more difficult, especially due to the crown surface diversity. From this point of view, it can be assumed that the model of finding the optimal vehicle path through the deciduous forest will be less reliable. The success of these models will largely depend on the resolution, coverage, and actuality of LiDAR data, as well as on the accuracy of the forest fire localization data. It should be noted that the use of this methodology in practice has a number of limitations resulting from data that cannot include all objects in the forest, such as lying trees, stones, low tree branches, etc. [34].

Tree branches can be an important obstacle to the movement of rescue vehicles. It mainly concerns young forests or deciduous forests, where branches are thicker and located below the ground. In coniferous stands, the lower branches of older trees are dry and thin and do not represent a major obstacle for heavy wheeled or tracked vehicles. Below is Table 1, containing measured data of tree branching; the lowest branches were about 1–2 cm thick. The measurement of tree canopy branching was performed only on trees for which resistance tensile forces were measured, not on all the trees in the area.

The problem is how to get the lower branch data. For this purpose, we plan to use LiDAR data with a resolution in cm [35–37] and use the last but one reflection for this measurement. Additionally, terrestrial LiDAR could help to solve this problem—we tested it on a small area in March 2022—see Figure 11 below.

The author assumes that, in the near future, it will be possible to solve the coordinates of trees, their *DBH*, and the characteristics of tree crown branches.

The spread of fire, depending on a number of factors, can be very variable, and actual data from burning areas will not always be available. Additionally, visibility can be significantly affected by smoke and the daytime. It should be noted that the calculation of the optimal vehicle route was based on the width of the vehicle. The reliability of route determination also depends on other vehicle parameters, such as vehicle length and height and minimum turning radius. This model did not even include a case where the vehicle would go back (e.g., in case of a spreading fire). For the more accurate calculations

of a vehicle route, the impact of the side slope should be also considered. Notable was also the driver's ability to overcome difficult terrain and to maneuver between trees in crisis situations.

Table 1. Branch position of selected trees.

Tree Num.	Tree Stem Diameter *DBH* (cm)	Height of Dry Branches (cm) (ϕ 1–2 cm)	Height of Semi-Dry Branches (cm)	Height of Green Branches (cm)	Tree Height (cm)
1	21.0	310	820	1080	1750
2	19.5	350	800	1040	1600
3	12.8	460	690	950	1460
4	19.0	490	870	1150	1730
5	13.9	none	720	930	1590
6	17.0	230	450	990	1710
7	17.8	380	510	650	1710
8	12.4	550	850	920	1470
9	22.1	170	500	1030	1730
10	18.3	330	770	900	1640
11	19.0	400	570	840	1640
12	16.7	560	830	970	1620
13	25.3	360	830	960	2050
14	23.7	none	340	1040	1870
15	22.9	350	550	930	1730
16	15.3	none	370	780	1525
17	14.3	260	470	750	1490
18	22.0	280	580	770	1550
19	10.8	none	380	650	1100
20	10.5	none	320	515	1030
21	14.5	770	990	1180	1770

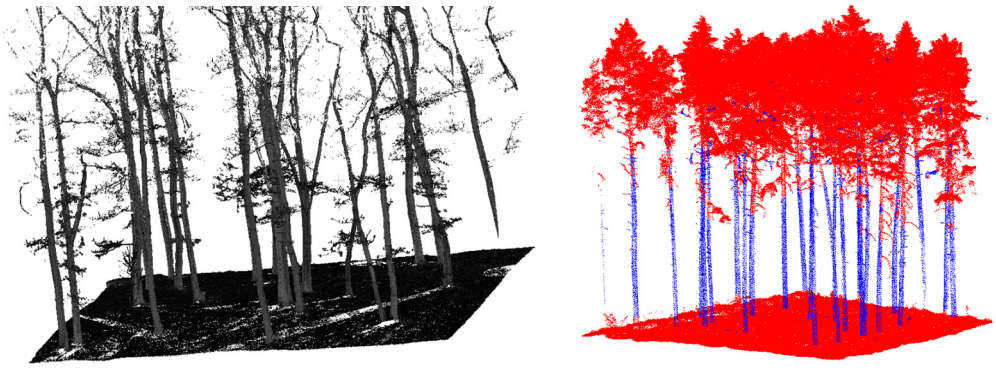

Figure 11. Deciduous and coniferous trees—segmentation of trunks and branches (crowns).

5. Conclusions

The primary aim of this article was to introduce the theoretical aspects, methods, and results of modeling the possibilities of firefighting rescue vehicle mobility in forest areas during fires using remote sensing data. The main result of the presented research is the methodology of the forest structure creation from DSM data, updating due to the growing vegetation parameters, as well as the proposal of the methodology of finding the optimum path of the vehicle to cross the forest, which is considerably more difficult than navigation on the roads.

Although the presented methods are approximate and their applications depend on a number of other factors, the author of the article believes that the presented methods and research results will be applicable in relation to the severity of damage caused by fire. The author also expects further developments of the vehicle navigation methodology in forest regions and the calculations of other factors influencing the search for optimal rescue

vehicle routes (low vegetation, lower branches of trees, inclination of slopes, soil influence, terrain surface, etc.). It will also be important to develop the theory and modeling of fire spread in forest areas and to link these models to rescue vehicle navigation.

Funding: This research received no external funding.

Institutional Review Board Statement: Not applicable.

Informed Consent Statement: Not applicable.

Data Availability Statement: Experimental data for Figure 2 and Table 1 were provided by Mendel University in Brno, for Figure 11 by the Czech Technical University in Prague and the Czech University of Life Sciences Prague.

Acknowledgments: This paper is the particular result of the defense research project DZRO VAROPS managed by the University of Defence in Brno, NATO-STO Support Project (CZE-AVT-2019), and specific research project 2021-23 at Department K-210 managed by the University of Defence, Brno.

Conflicts of Interest: The authors declare no conflict of interest. The funders had no role in the design of the study; in the collection, analyses, or interpretation of the data; in the writing of the manuscript; or in the decision to publish the results.

References

1. Vacchiano, G.; Foderi, C.; Berretti, R.; Marchi, E.; Motta, R. Modeling anthropogenic and natural fire ignitions in an inner-alpine valley. *Nat. Hazards Earth Syst. Sci.* **2018**, *18*, 935–948. [CrossRef]
2. Ganteaume, A.; Camia, A.; Jappiot, M.; San-Miguel-Ayanz, J.; Long-Fournel, M.; Lampin, C. A Review of the Main Driving Factors of Forest Fire Ignition Over Europe. *Environ. Manag.* **2012**, *51*, 651–662. [CrossRef]
3. Blair, J.; Rabine, D.L.; Hofton, M.A. The Laser Vegetation Imaging Sensor: A medium-altitude, digitisation-only, airborne laser altimeter for mapping vegetation and topography. *ISPRS J. Photogramm. Remote Sens.* **1999**, *54*, 115–122. [CrossRef]
4. Lim, K.; Treitz, P.; Wulder, M.; St-Onge, B.; Flood, M. LiDAR remote sensing of forest structure. *Prog. Phys. Geogr. Earth Environ.* **2003**, *27*, 88–106. [CrossRef]
5. Hyyppä, J.; Hyyppä, H.; Litkey, P.; Yu, X.; Haggrén, H.; Rönnholm, P.; Pyysalo, U.; Pitkänen, J.; Maltamo, M. Algorithms and methods of airborne laser scanning for forest measurement. *Int. Arch. Photogramm. Remote Sens.* **2004**, *36*, 82–89.
6. Aschoff, T.; Spiecker, H. Algorithms for the automatic detection of trees in laser scanner data. *Int. Arch. Photogramm. Remote Sens.* **2004**, *36*, 71–75.
7. Gobakken, T.; Næsset, E. Effects of forest growth on laser derived canopy metrics. *Int. Arch. Photogramm. Remote Sens.* **2004**, *36*, 224–227.
8. Carson, W.W.; Andersen, H.E.; Reutebuch, S.E.; McGaughey, R.J. Lidar Applications in Forestry—An Overview. In Proceedings of the ASPRS Annual Conference, Denver, Colorado, 24–28 May 2004.
9. Ahlberg, S.; Söderman, U.; Tolt, G. *High Resolution Environment Models from Sensor Data, In Defence Imagery Exploitation*; The United Kingdom's Ministry of Defence (MOD): London, UK, 2006.
10. Su, Y.; Guo, Q.; Fry, D.L.; Collins, B.M.; Jacob, M.K.; Flanagan, P.; Battles, J.J. A Vegetation Mapping Strategy for Conifer Forests by Combining Airborne Lidar Data and Aerial Imagery 2015. *Can. J. Remote Sens.* **2015**, *12*, 53. [CrossRef]
11. Martone, M.; Rizzoli, P.; Wecklich, C.; González, C.; Bueso-Bello, J.-L.; Valdo, P.; Schulze, D.; Zink, M.; Krieger, G.; Moreira, A. The global forest/non-forest map from TanDEM-X interferometric SAR data. *Remote Sens. Environ.* **2018**, *205*, 352–373. [CrossRef]
12. Kugler, F.; Schulze, D.; Hajnsek, I.; Pretzsch, H.; Papathanassiou, K.P. TanDEM-X Pol-InSAR Performance for Forest Height Estimation. *IEEE Trans. Geosci. Remote Sens.* **2014**, *52*, 6404–6422. [CrossRef]
13. Cazcarra-Bes, V.; Tello-Alonso, M.; Fischer, R.; Heym, M.; Papathanassiou, K. Monitoring of Forest Structure Dynamics by Means of L-Band SAR Tomography. *Remote Sens.* **2017**, *9*, 1229. [CrossRef]
14. Puletti, N.; Chianucci, F.; Castaldi, C. Use of Sentinel-2 for forest classification in Mediterranean environments. *Ann. Silvic. Res.* **2018**, *42*, 32–38. [CrossRef]
15. Gitas, I.Z.; Polychronaki, A.; Katagis, T.; Mallinis, G. Contribution of remote sensing to disaster management activities: A case study of the large fires in the Peloponnese, Greece. *Int. J. Remote Sens.* **2008**, *29*, 1847–1853. [CrossRef]
16. Milz, M.; Rymdteknik, A. *Study on Forest Fire Detection with Satellite Data*; Lulea Teknicka Universitet: Kiruna, Sweden, 2013; Available online: https://rib.msb.se/Filer/pdf/26593.pdf (accessed on 10 January 2022).
17. Koo, E.; Pagni, P.; Woycheese, J.; Stephens, S.; Weise, D.; Huff, J. A Simple Phisical Model for Forest Fire Spread Rate. *Fire Saf. Sci.* **2005**, *8*, 851–862. [CrossRef]
18. Ahlvin, R.B.; Haley, P.V. *NRMM II Users Guide*, 2nd ed.; Army Corps of Engineers; Procedural Guide for Preparation of DMA Cross-Country Movement (CCM) Overlays; Student handbook; DMA: Fort Belvoir, VA, USA, 1993; Volume 1.
19. Rybansky, M.; Vala, M. Analysis of relief impact on transport during crisis situations. *Morav. Geogr. Rep.* **2009**, *17*, 19–26.

20. Rybansky, M.; Hofmann, A.; Hubacek, M.; Kovarik, V.; Talhofer, V. Modelling of cross-country transport in raster format. *Environ. Earth Sci.* **2015**, *74*, 7049–7058. [CrossRef]
21. Rybansky, M.; Zerzán, P.; Břeňová, M.; Simon, J.; Mikita, T. Methods for the update and verification of forest surface model. In *International Archives of the Photogrammetry, Remote Sensing and Spatial Information Sciences—ISPRS Archives*; International Society for Photogrammetry and Remote Sensing: Praha, Czech Republic, 2016; pp. 51–54.
22. Rybansky, M.; Brenova, M.; Cermak, J.; Van Genderen, J.; Sivertun, Å. Vegetation structure determination using LIDAR data and the forest growth parameters. In Proceedings of the IOP Conference Series: Earth and Environmental Science, Kuala Lumpur, Malaysia, 13–14 April 2016; Volume 37, p. 12031.
23. Rybansky, M. Modelling of the optimal vehicle route in terrain in emergency situations using GIS data. In Proceedings of the IOP Conference Series: Earth and Environmental Science, Kuching, Malaysia, 26–29 August 2013; Volume 18, p. 12131.
24. Parsakhoo, A.; Jajouzadeh, M. Determining an optimal path for forest road construction using Dijkstra's algorithm. *J. For. Sci.* **2016**, *62*, 264–268. [CrossRef]
25. Fatehi, P.; Damm, A.; Leiterer, R.; Bavaghar, M.P.; Schaepman, M.E.; Kneubühler, M. Tree Density and Forest Productivity in a Heterogeneous Alpine Environment: Insights from Airborne Laser Scanning and Imaging Spectroscopy. *Forests* **2017**, *8*, 212. [CrossRef]
26. Matthews, R.W.; Jenkins, T.A.R.; Mackie, E.D.; Dick, E.C. *Forest Yield: A Handbook on Forest Growth and Yield Tables for British Forestry*; Forestry Commission: Edinburgh, Scotland, 2016; pp. 1–92, ISBN 978-0-85538-942-0.
27. Rybansky, M. *The Cross–Country Movement—The Impact and Evaluation of Geographic Factors*; CERM: Brno, Czech Republic, 2009; p. 113, ISBN 978-80-7204-661-4.
28. Simon, J.; Kadavý, J.; Macků, J. *Forest Economic Adjusting*; MZLÚ: Brno, Czech Republic, 1998. (In Czech)
29. Hubacek, M.; Kovarik, V.; Kratochvil, V. Analysis of Influence of Terrain Relief Roughness on Dem Accuracy Generated from Lidar in the Czech Republic Territory. *ISPRS Int. Arch. Photogramm. Remote Sens. Spat. Inf. Sci.* **2016**, *XLI-B4*, 25–30. [CrossRef]
30. Cibulová, K.; Sobotková, Š. Different Ways of Judging Trafficability. *Adv. Mil. Technol.* **2006**, *1*, 77–87.
31. Hošková-Mayerová, S.; Talhofer, V.; Hofmann, A. Mathematical modell used in decision-making process with respect to the reliability of geo database. *Procedia Soc. Behav. Sci.* **2010**, *9*, 1652–1657. [CrossRef]
32. Stodola, P.; Mazal, J. Optimal Location and Motion of Autonomous Unmanned Ground Vehicles. *WSEAS Trans. Signal Processing* **2010**, *6*, 68–77.
33. Pokonieczny, K. Automatic military passability map generation system. In Proceedings of the International Conference on Military Technologies (ICMT), Brno, Czech Republic, 31 May–2 June 2017; pp. 285–292.
34. Abdullahi, S.; Kugler, F.; Pretzch, H. Prediction of stem volume in complex temperate forest stands using TanDEM-X SAR data. *Remote Sens. Environ.* **2016**, *174*, 197–211. [CrossRef]
35. Štroner, M.; Urban, R.; Línková, L. A New Method for UAV Lidar Precision Testing Used for the Evaluation of an Affordable DJI ZENMUSE L1 Scanner. *Remote Sens.* **2021**, *13*, 4811. [CrossRef]
36. Surový, P.; Kuželka, K. Acquisition of Forest Attributes for Decision Support at the Forest Enterprise Level Using Remote-Sensing Techniques—A Review. *Forests* **2019**, *10*, 273. [CrossRef]
37. Krůček, M.; Král, K.; Cushman, K.; Missarov, A.; Kellner, J.R. Supervised Segmentation of Ultra-High-Density Drone Lidar for Large-Area Mapping of Individual Trees. *Remote Sens.* **2020**, *12*, 3260. [CrossRef]